Lattice distortions and local compressibility around trivalent rare-earth impurities in fluorites

M. Tovar, C. A. Ramos, and C. Fainstein
Centro Atómico Bariloche, Comisión Nacional de Energía Atómica, and Instituto Balseiro, Universidad Nacional de Cuyo, 8400 Bariloche, Argentina
(Received 8 March 1983)

We have calculated the lattice distortions around trivalent rare-earth dilute impurities, occupying substitutionally metal sites in fluorites. Explicit results are given for the equilibrium positions of the nearest fluorine ligands, R, the induced electric dipole moments, and the local hydrostatic strains for MF_2 (M=Cd, Ca, Sr, Pb, and Ba). These results are used to study the impurity-ligand distance dependence of the fourth-order cubic-crystal-field parameter, b_4, for Gd^{3+} and the isoelectronic ion Eu^{2+}. Comparison is made with the change of b_4 with hydrostatic stress using the calculated local compressibility of the lattice. A consistent description of the experimental data is obtained assuming $b_4 \propto R^{-m}$ with $m \sim 10$.

INTRODUCTION

The analysis of microscopic properties of dilute paramagnetic ions in solids, such as the crystal field or the transferred hyperfine interactions, requires the knowledge of the actual position of the ligand ions. These are displaced from the regular sites of the perfect lattice, and their actual equilibrium positions can be estimated through a minimization of the cohesion energy of the impure crystal.

In a previous paper,[1] hereafter called I, we studied the local distortions for the case of divalent thulium impurities in fluorite-type lattices. We report here the extension of our model to the case of trivalent rare-earth impurities, where the excess charge produces important changes in their neighborhood. The results are used to correlate the crystal-field parameters for Gd^{3+} (and Eu^{2+}) in different fluorites with the calculated equilibrium positions of the ligand ions. The functional dependence obtained is compared with experimental data on the crystal-field changes with an externally applied hydrostatic pressure, taking into account the local compressibility of the lattice.

LATTICE DISTORTIONS

The local distortions around substitutional trivalent rare-earth impurities in MF_2 (M=Cd, Ca, Sr, Pb, and Ba) have been calculated by allowing radial ionic displacements up to the eighth coordination sphere, in order to minimize the cohesion energy of the lattice with the impurity. This was accomplished, as in I, within the framework of a shell model[2] where ions are described by a core of charge $X|e|$ and an electron shell of charge $Y|e|$, $Z|e| = X|e| + Y|e|$ being the net ionic charge. For the shell charges we have used here the revised estimates given in Ref. 3, assuming for F^-, Ca^{2+}, Sr^{2+}, and Ba^{2+} the values calculated for the isoelectronic rare gases, i.e., $Y=-2.40$, -4.35, -4.95, and -5.65, respectively. For Cd^{2+} and Pb^{2+} the values $Y=-5.45$ and -6.35 were obtained by interpolation according to atomic number. Values for the electronic polarization of the metal ions, $\alpha_M = 1.33$ and 3.41 Å^3 for CdF_2 and PbF_2, respectively, have been estimated from dielectric constant data[4,5] using the relation

$$\alpha_M + 2\alpha_F = (3a^3/16\pi)[(\epsilon_\infty - 1)/(\epsilon_\infty + 2)] \ ,$$

where a is the lattice parameter. The electronic polarizability of the F^- ions has been taken equal to the average of the values given by Sharma *et al.*[6] for the alkaline-earth fluorides: $\alpha_F = 0.80$ Å^3.

As was described in detail in I, the cohesion energy has Coulomb and short-range contributions as well as terms associated with the formation of induced electric dipoles on the ions surrounding the impurity. For the short-range interactions we have used here Born-Mayer potentials, $V(r) = A\exp(-r/\rho)$, whose coefficients have been determined from the elastic constants of the pure lattices.[2] For CaF_2, SrF_2, and BaF_2 we have used the values of the potential derivatives given in I, and for CdF_2 and PbF_2 those listed in Table I. Potentials for the rare-earth–fluorine interaction were obtained by Kimble *et al.*[7] from dielectric relaxation data on rare-earth doped fluorites in the case of Sm^{3+}, Eu^{3+}, Gd^{3+} and Tb^{3+}. The values of other trivalent rare earths shown in Table II have been extrapolated assuming a relation between A and the ionic radius of the rare-earth ions, r_i, given by

$$A_i \propto (r_i + r_F)^{-2}\exp[(r_i + r_F)/\rho] \ ,$$

where r_F is the F^- ionic radius; $\rho = 0.2997$ Å was used for all rare earths as in Ref. 7. This dependence for A is consistent with ligand distances equal to the sum of the ionic radii, $r_i + r_F$, in ionic rare-earth trifluorides, if short-range interactions between fluorine ions are not considered. For the F^--F^- short-range interaction we have used a Buckingham potential,[8]

$$V_{--}(r) = A_{--}\exp(-r/\rho_{--}) - C_{--}/r^6 \ ,$$

TABLE I. Lattice parameter and elastic constants for CdF_2 and PbF_2, at 4.2 and 10 K, respectively.

	CdF_2[a]	PbF_2[b]
a (Å)	5.365	5.902
C_{11} (10^{11} dyn cm^{-2})	19.79	10.91
C_{12} (10^{11} dyn cm^{-2})	7.294	5.45
C_{44} (10^{11} dyn cm^{-2})	2.490	2.37

[a]D. O. Pederson and J. A. Brewer, Phys. Rev. B 16, 4546 (1977).
[b]M.H. Dickens and M. T. Hutchings, J. Phys. C 11, 461 (1978).

TABLE II. Born-Mayer potentials for metal-fluorine short-range interaction $V(r)=A\exp(-r/\rho)$; $\rho=0.2997$ Å for all trivalent rare-earth ions.

	A (eV)	ρ (Å)		A (eV)		A (eV)
Cd^{2+}	7835	0.2334	Ce^{3+}	2965	Tb^{3+}	2251[a]
Ca^{2+}	1918	0.2805	Pr^{3+}	2813	Dy^{3+}	2174
Sr^{2+}	3100	0.2794	Nd^{3+}	2691	Ho^{3+}	2101
Pb^{2+}	4246	0.2763	Sm^{3+}	2488[a]	Er^{3+}	2036
Ba^{2+}	5252	0.2792	Eu^{3+}	2408[a]	Tm^{3+}	1978
Eu^{2+}	3384	0.2770	Gd^{3+}	2349[a]	Yb^{3+}	1926

[a]Reference 7.

that describes the existence of two force regions, one attractive and the other repulsive. The values $A_{--}=4370$ eV, $C_{--}=144$ eV Å^6, and $\rho_{--}=0.2753$ Å, have been chosen to fit the measured values of the elastic constants of the fluorites considered in this paper.

Values for the equilibrium positions of the rare-earth ligands have been obtained following an iterative method of calculus, where the cohesion energy is successively expanded up to second order in the ionic displacements around positions that converge from the perfect lattice sites toward the final equilibrium distances. We have found that this point is of fundamental importance in the case of heterovalent substitution, where the distortions reach values close to 10% of the lattice parameter due to the excess charge on the impurities. As an example, we show in Table III the results obtained at intermediate iteration steps for Gd^{3+} in BaF_2. Here, the final equilibrium positions differ significantly from the values obtained in the first step where the energy was expanded around the perfect lattice sites.

These differences are even greater when considering local strains, which are associated with the curvature of the potential at the equilibrium positions. For the large lattice distortions found for trivalent rare-earth impurity ions, the assumption of curvature independent of ionic position[1,9] is no longer valid, and important changes are expected. Actually, in cases such as the one shown in Table III this approximation predicts a local softening of the lattice, while the final result of our calculation is a considerable hardening.

In Fig. 1 we display the calculated nearest-neighbor equilibrium positions, the induced electric dipoles, and the ratio between local and macroscopic hydrostatic strains. These values have been obtained by allowing up to eight coordination spheres around the impurity to relax to new equilibrium positions. The need for this is seen in Fig. 2, where we show the change in the calculated equilibrium position for the nearest ligands as a function of the number of relaxed coordination spheres.

TABLE III. Equilibrium position R, and hydrostatic local strain e_1/e for nearest neighbors in Gd^{3+}:BaF_2, when expanding about R_0 at the nth step of the calculation. Changes in R are typically smaller than 0.1% after the third iteration.

n	R_0 (Å)	R (Å)	e_1/e
1	2.675	2.199	1.609
2	2.437	2.404	
3	2.404	2.408	
4	2.408	2.408	0.632

CRYSTAL FIELD FOR Gd^{3+}

In the case of Gd^{3+} ions occupying substitutionally cubic sites, the crystal field for the ground state ($4f^7\,{}^8S_{7/2}$) is described by just two parameters[10]: b_4 and b_6. Comparison of experimental values of b_4, from electron paramagnetic resonance (EPR) experiments in different lattices, indicates an R^{-m} dependence on the metal-fluorine distance R. Assuming for R the same values as in the perfect lattices, $m\sim2$ is obtained for Gd^{3+} in fluorites,[11] while $m\sim4$ results for the isoelectronic ion Eu^{2+} in the same lattices.[11,12] These values of m are at variance with those obtained from hydrostatic stress experiments[13,14]: $m\sim7$ for Gd^{3+} and $m\sim9$ for Eu^{2+}. In a detailed study of the correlation between crystal-field parameters and ligand distances, Edgar and Newman[15] concluded that the inconsistency of these results is related to the local lattice distortions and the changes in local compressibility. However, their use of the equilibrium distances calculated by Ivanenko and Malkin[9] did not improve the correlation and the need for more detailed calculations of local distortions was suggested.

In this paper we compare b_4 for Gd^{3+} and Eu^{2+} in cubic sites of different fluorite lattices as a function of our calculated equilibrium distances, listed in Table IV. (The values reported here for Eu^{2+} differ slightly from those obtained in I due to the iterative process introduced in the present calculation.)

As shown in Fig. 3, b_4 closely follows a monotonically decreasing function of the calculated equilibrium distances for both Gd^{3+} and Eu^{2+}. The only exception is Eu^{2+} in CdF_2 where the measured value might indicate a larger lattice distortion. However, the importance of different contributions to b_4 in this case cannot be ruled out since CdF_2 has not the same electronic structure as the alkaline-earth fluorides. The calculated logarithmic slopes are very similar for both ions: $m=9.7$ for Gd^{3+}, and $m=9.6$ for Eu^{2+}, if the value for Eu^{2+}:CdF_2 is not considered. The inclusion of this point would lead to $m=7.9$.

Hydrostatic[13,14,16,17] and uniaxial[18–21] stress experiments provide independent information on the ligand distance dependence of b_4, when appropriate values for the local compressibility are known. Using our calculated values for the local strain and the data on db_4/dP listed in Table V we obtained values of m averaging 10, with Eu^{2+} in BaF_2 being the only significant deviation. This case, however, must be treated with caution since the fitting of the EPR spectra[14] indicates also surprisingly large changes with pressure in both the hyperfine structure constant A and the sixth-order crystal-field parameter b_6.

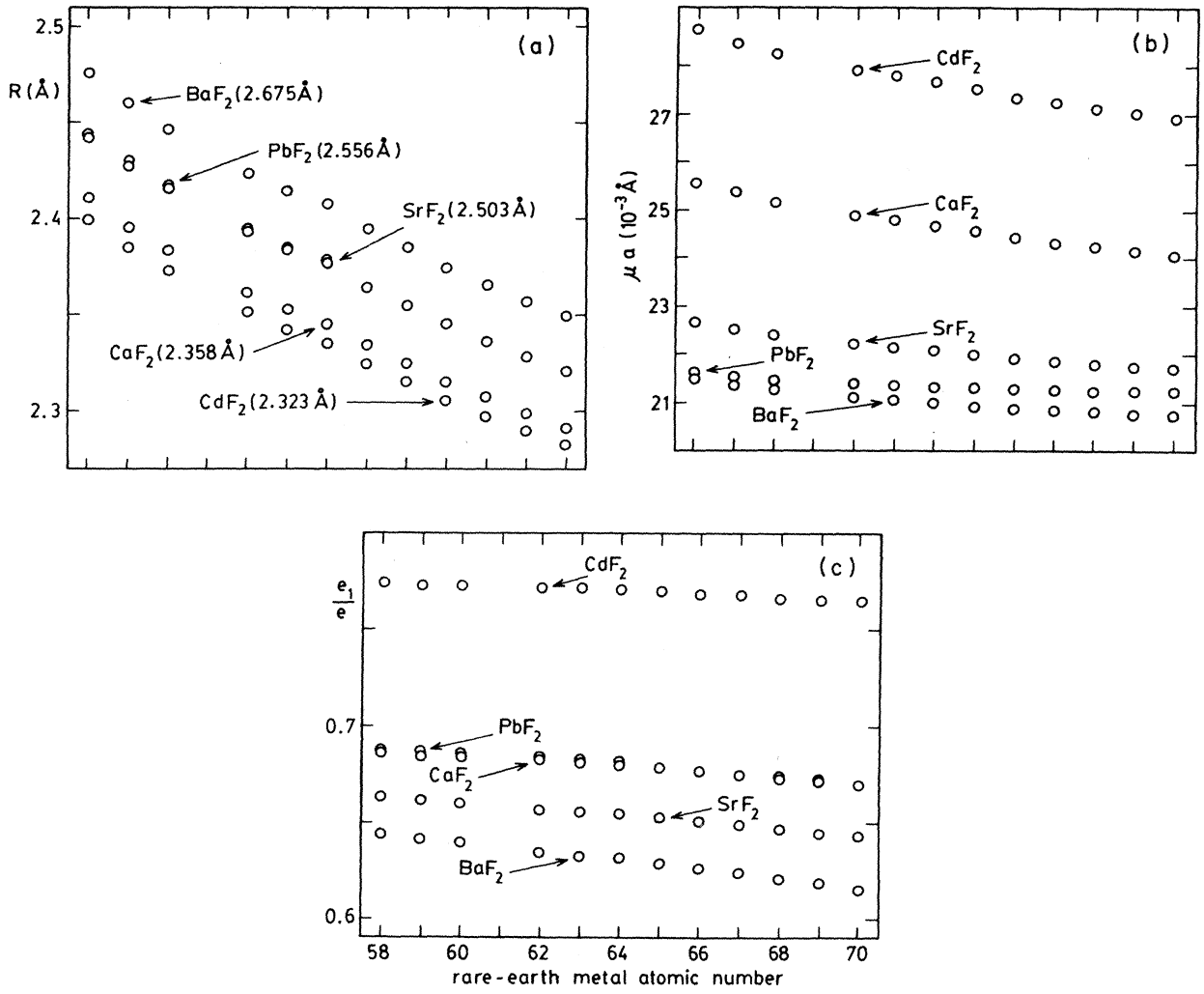

FIG. 1. Calculated impurity-ligand distance R, induced electric dipole moments $\vec{D} = -Y_F |e| \mu a \vec{R}/|\vec{R}|$, and local hydrostatic strain e_1/e for the trivalent rare-earth ions. Numbers in parentheses are the corresponding perfect lattice distances in Å.

TABLE IV. Crystal-field parameter b_4 in units of 10^{-4} cm^{-1}, extrapolated at 0 K, and calculated equilibrium positions R.

	Gd^{3+}		Eu^{2+}	
Host	R (Å)	$-b_4$	R (Å)	$-b_4$
CdF_2	2.336	50.45(1)[a]	2.432	56.3(3)[f]
CaF_2	2.346	48.6(3)[b]	2.454	58.75(1)[g]
SrF_2	2.377	42.3(2)[c]	2.507	47.6(5)[h]
PbF_2	2.375	43.3(1)[d]	2.507	
BaF_2	2.408	37.75(8)[e]	2.566	38.3(5)[h]

[a]R. H. Borchert, T. Cole, and T. Horn, J. Chem. Phys. 49, 4880 (1968).
[b]K. Horai, J. Phys. Soc. Jpn. 19, 2241 (1964).
[c]M. M. Abraham and L. A. Boatner, J. Chem. Phys. 51, 3134 (1969).
[d]J. M. Baker and R. L. Wood, J. Phys. C 12, 4033 (1979).
[e]L. A. Boatner, R. W. Reynolds, and M. M. Abraham, J. Chem. Phys. 52, 1248 (1970).
[f]Reference 12.
[g]J. M. Baker and F. I. B. Williams, Proc. London Soc. 267, 283 (1962).
[h]T. Rewaj, Fiz. Tverd. Tela (Leningrad) 9, 2978 (1967) [Sov. Phys.—Solid State 9, 2340 (1968)].

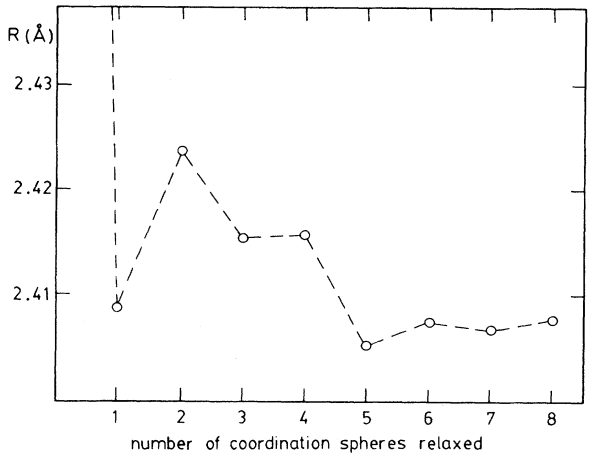

FIG. 2. Calculated impurity-ligand distance in Gd^{3+}:BaF_2 as a function of the number of coordination spheres allowed to relax.

In conclusion, we have shown that it is possible to obtain a high degree of internal consistency on the analyzed body of experimental data with $b_4 \propto R^{-m}$ ($m \sim 10$) using our calculated values for the equilibrium distances and local strains. We have not attempted to make a similar correlation for b_6 due to the scatter of the available experimental data.

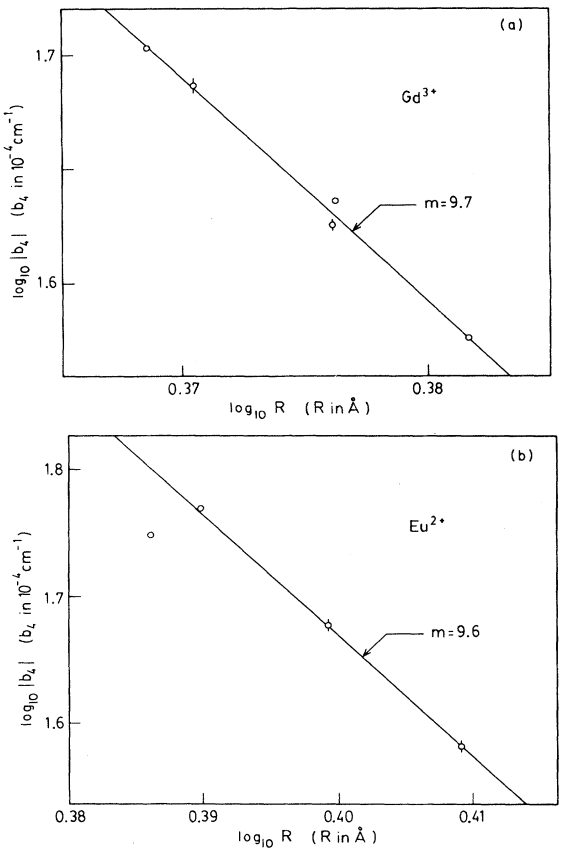

FIG. 3. Fourth-order crystal-field parameter b_4 vs calculated impurity-ligand distance.

TABLE V. Pressure derivatives of b_4 in hydrostatic (P_h) and uniaxial (P_u) stress experiments, in units of 10^{-4} cm^{-1}/kbar, calculated local hydrostatic strains e_1/e, and exponent m corresponding to $b_4 \propto R^{-m}$.

	CdF_2	CaF_2	SrF_2	BaF_2
		Gd^{3+}		
$\frac{db_4}{dP_h}$	0.142[a]	0.133(13)[d]	0.128(20)[d]	0.158(13)[d]
$\frac{db_4}{dP_u}$	0.09(5)[b]	0.12(4)[b]		
	0.20(16)[c]			
e_1/e	0.798	0.708	0.685	0.683
m	12.0	10(1)	9.3(1.4)	9.9(8)
		Eu^{2+}		
$\frac{db_4}{dP_h}$	0.164[e]	0.201(20)[g]	0.205(16)[g]	0.140(21)[g]
$\frac{db_4}{dP_u}$	0.16(5)[f]	0.19(15)[h]		
e_1/e	1.041	0.941	0.991	1.074
m	10.0	10(1)	9.7(8)	6.1(9)

[a]Reference 16.
[b]Reference 18.
[c]Reference 19.
[d]Reference 13.
[e]Reference 17.
[f]Reference 20.
[g]Reference 14.
[h]Reference 21.

The parameters b_4 and b_6 are coefficients of the spin Hamiltonian describing the splitting of the ground state $^8S_{7/2}$ of the configuration $4f^7$. Similar parameters can be defined for the excited states, and their correlation with the ion-ligand distance has been analyzed in Ref. 22 for the multiplets $^6P_{7/2}$ and $^6P_{5/2}$ of Gd^{3+} in CaF_2, SrF_2, and BaF_2. Their results for the fourth-order term correspond to slopes $m=12.9$ and -1.8, if our values for R are used.

Relating all these phenomenological parameters to microscopic crystal-field interactions requires the knowledge of the particular perturbation mechanism that gives rise to the observed splittings. The electronic configuration $4f^7$ is a half-filled shell, and thus all the diagonal crystal-field matrix elements are zero between pure Russel-Saunders coupled states. It is then essential to completely diagonalize the free-ion Hamiltonian including spin-orbit, spin-spin, spin-other-orbit, and configuration interactions in order to obtain intermediate coupled wave functions that could explain the observed nonzero splittings. This was done in Refs. 22 and 23, and the authors found that a simple first-order perturbation mechanism in the microscopic crystal-field interaction H_{cf} cannot simultaneously explain the observed splittings for the $^8S_{7/2}$, $^6P_{7/2}$, and $^6P_{5/2}$ states or their different impurity-ligand distance dependence. Instead, a full diagonalization of H_{cf} with the lowest fifteen free-ion multiplets was required in order to obtain a reasonable fit of the optical spectra of the $^6P_{7/2}$ and $^6P_{5/2}$ states. The microscopic crystal-field parameter $A_4\langle r^4\rangle$ estimated in this way follows an impurity-ligand distance dependence with a logarithmic slope $m=8.6$, if again our results for R are used. This value is close to the slope $m\cong 10$ we have obtained for the $^8S_{7/2}$ ground-state splitting, as might be expected since almost 80% of the calculated splitting for the $^8S_{7/2}$ ground state in Ref. 23 was obtained from a first-order perturbation mechanism. A more detailed study of the relation between the microscopic and phenomenological crystal-field parameters for Gd^{3+} and Eu^{2+} would require a critical analysis of the ground-state free-ion eigenvectors, which is beyond the scope of this paper.

ACKNOWLEDGMENTS

This work was supported in part by the Consejo Nacional de Investigaciones Científicas y Técnicas (Argentina), as were two of us (M.T. and C. A. Ramos), and in part by the Multinational Program of the Organization of American States.

[1]C. Fainstein, M. Tovar, and C. Ramos, Phys. Rev. B 25, 3039 (1982).
[2]J. D. Axe, Phys. Rev. 139, A1215 (1965).
[3]B. G. Dick, Phys. Rev. 145, 609 (1966).
[4]D. R. Bosomworth, Phys. Rev. 157, 709 (1967).
[5]G. A. Samara, Phys. Rev. B 13, 4529 (1976).
[6]J. C. Sharma, H. P. Sharma, and Jai Shanker, J. Chem. Phys. 67, 3642 (1977).
[7]R. J. Kimble Jr., Peter J. Welcher, John J. Fontanella, Mary C. Wintersgill, and Carl G. Andeen, J. Phys. C 15, 3441 (1982).
[8]C. R. A. Catlow and M. J. Norgett, J. Phys. C 6, 1325 (1973).
[9]Z. I. Ivanenko and B. Z. Malkin, Fiz. Tverd. Tela (Leningrad) 11, 1857 (1969) [Sov. Phys.—Solid State 11, 1498 (1970)].
[10]M. T. Hutchings, in *Solid State Physics,* edited by F. Seitz and D. Turnbull (Academic, New York, 1964), Vol. 16, p. 227.
[11]R. S. Title, Phys. Lett. 6, 13 (1963).
[12]H. J. Gläser and D. Gerst, Z. Naturforsch. 239, 1980 (1968).
[13]S. V. Kasatochkin, T. I. Alaeva, E. N. Yakovlev, and L. F. Vereshchagin, Fiz. Tverd. Tela (Leningrad) 15, 312 (1973) [Sov. Phys.—Solid State 15, 229 (1973)].
[14]W. R. Hurren, H. M. Nelson, E. G. Larson, and J. H. Gardner, Phys. Rev. 185, 624 (1969).
[15]A. Edgar and D. J. Newman, J. Phys. C 8, 4023 (1975).
[16]T. Rewaj and M. Krupski, Phys. Status Solidi B 88, K65 (1978).
[17]T. Rewaj and M. Krupski, Phys. Status Solidi B 99, 285 (1980).
[18]S. B. Oseroff and R. Calvo, J. Phys. Chem. Solids 33, 2275 (1972).
[19]K. Falkowski, J. Szumowski, B. Krukowska-Fulde, and J. Jablonski, Phys. Status Solidi B 66, 63 (1974).
[20]J. Szumowski, K. Falkowski, B. Krukowska-Fulde, and A. Sienkiewicz, Phys. Status Solidi B 72, K121 (1975).
[21]J. Kuriata, N. Guskos, T. Rewaj, J. Szumowski, and K. Falkowski, Phys. Status Solidi B 74, 683 (1976).
[22]J. M. O'Hare, J. A. Detrio, and V. L. Donlan, J. Chem. Phys. 51, 3937 (1969).
[23]J. M. O'Hare and V. L. Donlan, Phys. Rev. 185, 416 (1969).